

Article

Accuracy Optimization for High Resolution Object-Based Change Detection: An Example Mapping Regional Urbanization with 1-m Aerial Imagery

Kenneth B. Pierce Jr.

WA Department of Fish and Wildlife, Habitat Science Division, 1111 Washington St SE, Olympia, WA 98501, USA; E-Mail: Kenneth.piercejr@dfw.wa.gov; Tel.: +1-360-902-2564; Fax: +1-360-902-2946

Academic Editors: Soe Myint and Prasad S. Thenkabail

Received: 14 May 2015 / Accepted: 18 September 2015 / Published: 25 September 2015

Abstract: The utility of land-cover change data is often derived from the intersection with other information, such as riparian buffers zones or other areas of conservation concern. In order to avoid error propagation, we wanted to optimize our change maps to have very low error rates. Our accuracy optimization methods doubled the number of total change locations mapped, and also increased the area of development related mapped change by 93%. The ratio of mapped to estimated change was increased from 76.3% to 86.6%. To achieve this, we used object-based change detection to assign a probability of change for each landscape unit derived from two dates of 1 m US National Agriculture Imagery Program data. We developed a rapid assessment tool to reduce analyst review time such that thousands of locations can be reviewed per day. We reviewed all change locations with probabilities above a series of thresholds to assess commission errors and the relative cost of decreasing acceptance thresholds. The resultant change maps had only change locations verified to be changed, thus eliminating commission error. This tool facilitated efficient development of large training sets in addition to greatly reducing the effort required to manually verify all predicted change locations. The efficiency gain allowed us to review locations with less than a 50% probability of change without inflating commission errors and, thus, increased our change detection rates while eliminating both commission errors and locations that would have been omission errors among the reviewed lower probability change locations.

Keywords: land-use/land-cover change; high resolution imagery; accuracy assessment; random forests; confusion matrix

1. Introduction

The simultaneous rise in land surface data availability, digital imaging technology, and inexpensive computational power since the turn of the millennium have the potential to greatly advance the developing fields of land-change [1,2] and urbanization science [3]. While encompassing remote sensing, scientists from both disciplines are particularly interested in examining coupled human–ecosystem interactions and applying land-cover/land-use (LCLU) mapping and change data to managing and perpetuating ecosystem services [4–7]. New space-based platforms, such as IKONOS (1 m), SPOT5 (2.5–5 m), QuickBird (0.6–2.4 m), and WorldView (1–2 m), as well as plane-based aerial imaging (0.1–2 m), have extensively increased the amount of high resolution digital imagery available to researchers and policy makers worldwide [8–12].

Analytical techniques for this data were largely developed with lower resolution imagery, such as Landsat (30 m) and MODIS (250 m) data, and a great deal of debate remains as to whether those techniques apply well to data with smaller pixel sizes [13,14]. In the past decade, geographic object based image analysis (GEOBIA) and object based change detection (OBCD) have increasingly been used to map land cover and land cover change with these higher resolution data types by grouping the pixels back into whole landscape features [15–17]. With OBCD, pixels are grouped into polygon objects for analysis rather than being treated individually. Object-based image analysis has been an important step in bridging the gap between the extensive analytical power of pixel-based image analysis and the decades-old practice of air photo interpretation, which has been vital to regional land managers and policy makers since the 1940s [13,18–20].

However, while object-based techniques have helped with image interpretation, applying this data to the assessment of coupled human–ecosystem interactions requires integrating multiple data types [21]. Data mismatches may occur among raster images from potentially different sources and/or times [22–24], and vector GIS data, such as parcel boundaries, stream lines, zoning data, building footprints [25–27], and point data, such as locations of toxic sources, building permits, or species observations [28], may all contain positional and attribute error. In addition to the scaling issues across different data sets [29,30], error in individual data sources compounds overall model errors when multiple data sets are integrated [31,32].

1.1. Objectives

The primary objective of this paper is to present a set of techniques that seek to optimize the accuracy of object-based change detection results so that they can be integrated with other data sets with minimal error inflation and, thus, aid applications such as effectiveness monitoring and informing land management issues [15,33–35]. Those techniques include: (i) a procedure for substantially eliminating commission error in mapped change locations through efficient error checking; (ii) a process that supports lowering change prediction thresholds to increase the mapped change area while

decreasing omission errors; and (iii) a software system to facilitate the presented techniques. These techniques are applied after typical accuracy assessment procedures [36,37] such that they could be used to increase the accuracy of existing studies employing object-based change detection.

1.1.1. Object-Based Image Analysis and Change Detection

Object-based image analysis methods (GEOBIA/OBIA) are frequently being used to map land-cover and land-cover change when the pixel size of the imagery is small relative to the individual extents of common landscape features [35,38–40]. In urban and rural landscapes, many features are smaller than the 30-m extent of Landsat pixels and are, thus, better resolved with higher resolution imagery, such as that provided by the previously-mentioned space-based platforms or aerial imaging. OBIA methods group pixels into homogenous units based on local variance criteria [15,33,41,42]. Once the pixels are converted to segments, many classification and change detection techniques, designed for pixel-based analyses, can be applied to the segments [5,43,44]. Change detection has two main methods, post-classification change detection and combined change detection [45,46]. Post-classification change mapping considers the differences between two individual classified maps at different times and inherently combines individual mapping errors [47]. A combined change detection analyzes the two times simultaneously, by assessing the differences or correlations between reflectance values of the two images [16,48]. In accordance with these two methods, the former often leads to maps of explicit class-to-class changes, while the latter simply maps areas as changed/not-changed.

1.1.2. Accuracy Assessment

Map accuracy is characterized in terms of positional and thematic accuracy [36]. High resolution imagery can be well registered because man-made and natural landmarks lead to visual verification for change events [5]. Thematic accuracy of a classification or change model is usually assessed by calculating the prediction efficiency for some withheld or newly collected training data [36,49–51]. For a simple change classifier, observed locations can be mapped as having (1) changed; (2) not changed; (3) changed erroneously; or (4) not changed erroneously. Counts of these quantities are displayed in a confusion matrix with the main diagonal elements representing correctly classified observations [36,52] and the non-zero off-diagonal counts representing the two types of errors (Figure 1). Locations labeled as change erroneously are the commission errors, while erroneous non-changed locations (locations that actually did change but were not mapped as such) are the omission errors.

The job of a statistical classifier is to find a set of attributes that minimizes these classification errors [53]. However, these types of errors are not always viewed with equal weight. In the language of receiver operating curves, a classifier has a high sensitivity (is called a liberal classifier) if it correctly classifies a high percentage of observed changes [37]. A classifier that correctly attributes non-changing observations has a high specificity or is referred to as a conservative classifier. High sensitivity usually comes with higher commission errors and high specificity is accompanied by more omission errors. Therefore, there is a tradeoff for optimizing a classifier for either sensitivity or specificity [37]. Optimization is achieved by altering the minimum accepted threshold for labeling an analysis unit as a certain class. The simple threshold is usually 50% for a two class model or the

reciprocal of the number of classes for models with more than two classes. When the risks associated with the two types of error are not equal, thresholds can be altered to minimize the cumulative risk instead of the simple error rate.

		Actual Change Status	
		Changed	No Change
Modeled Change Status	Changed	Correctly Classified	Commission Errors
	No Change	Omission Errors	Correctly Classified

Figure 1. Confusion matrix for mapping land cover change.

Combined change detection uses a threshold set on some image difference across times, such as overall brightness, to assess how much of a difference is enough to be considered a change. For example, in a recent paper on high resolution change detection [54], the authors suggested using the distribution of the normalized difference vegetation index (NDVI) differences between dates as a measure for change, specifically, they suggested using the standard deviation as a threshold for assigning a polygon as changed. Setting a high threshold will mean less area will be mapped as change, but should have lower commission errors and, thus, higher omission errors. Conversely, setting a low difference threshold, accepting a low probability of change as change-should capture more change, but will also increase the erroneous area of mapped change, *i.e.*, commission errors.

1.1.3. Accuracy Optimization

Our two proposed accuracy optimization techniques are designed to use accuracy assessment information to optimize the overall accuracy of the final map product by ensuring verified mapped change locations and removal of erroneously mapped changes. The purpose of the first technique we propose is to eliminate commission errors in change maps. To achieve this, all locations predicted to have changed need to be verified. Since manual photo interpretation is routinely used as “ground truth” data, our process includes photo interpretation of all predicted change locations, in as much as each photo is viewed by an analyst and the presence of an anthropogenic or natural disturbance is noted. With this approach to error characterization all commission errors occur within the predicted change area while all the omission errors remain in the predicted non-change area. The area of predicted change is generally much smaller than the non-change area for the landscapes we are working in over our two- to three-year imagery intervals. Therefore, the task of interpreting just the locations with potential commission error is much smaller than the task of interpreting locations of potential omission error.

The second technique described here is made possible as a result of interpreting all the predicted changes. For a binary model, logistic regression for example, predicted changes are those for which the model assigns change as the most probable class. With a two class model, 50% is the minimum prediction threshold for assigning an analysis unit to the change category. As previously stated, the problem with lowering this minimum acceptance probability is increasing the model's commission errors. Since we check all potential commission errors, this threshold can be lowered at a cost of additional interpretation time as opposed to increased model error. As the threshold is lowered, additional photo interpretation effort will increase. Thus, the optimal threshold is somewhere between 0 and 50%.

2. Methods

2.1. Study Area

Our study covers one of the 19 major watersheds in the Puget Sound region of the state of Washington in the Northwestern United States. The watershed encompasses the Puyallup river basin and ranges from the city of Tacoma, WA, at sea level to the top of Mount Rainier (Figure 2). It covers 272,932 ha with an elevation range from 0 to 4394 m. National Parks and National Forests make up just over 40% of the total area, occupying the upper range of elevations.

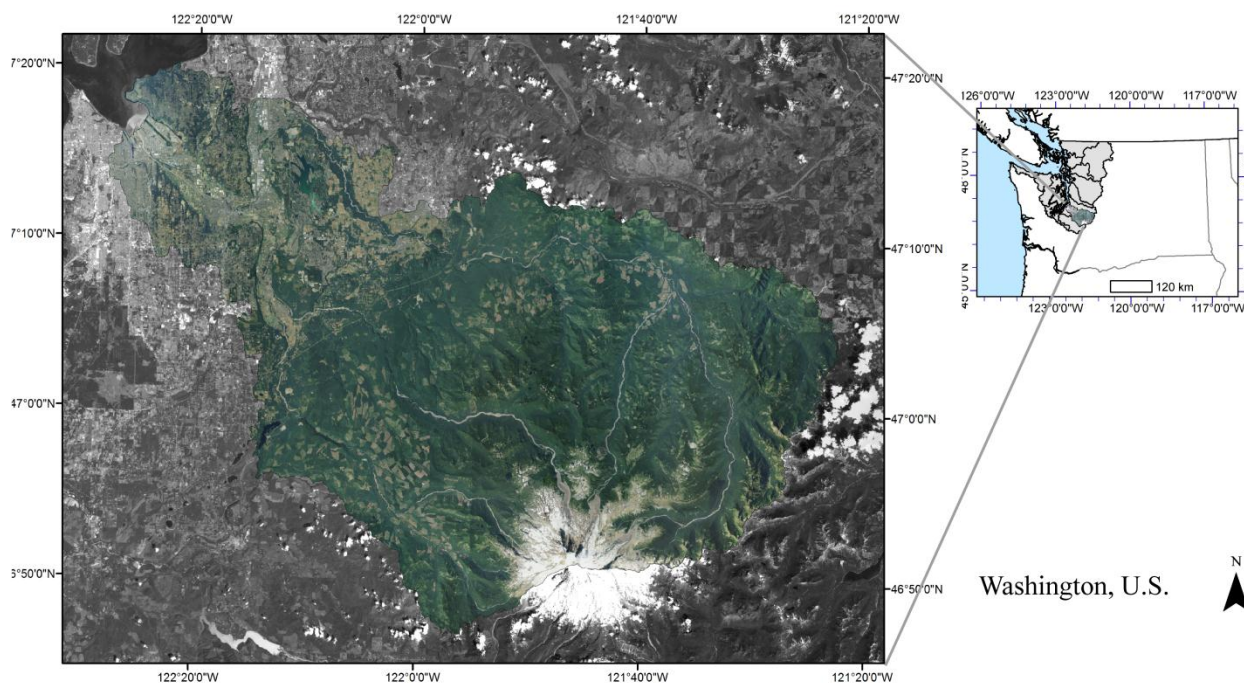


Figure 2. The Puyallup watershed is one of 19 watersheds making up the Puget Sound region of Washington State. The watershed covers 272,932 ha and rises from the city of Tacoma at sea level up to the top of Mt. Rainier at 4394 m.

On an annual basis, the urbanization change rate in the Puget Sound region is small. For example, the US National Oceanographic and Atmospheric Administration's Coastal Change and Analysis Program data showed that from 1992 to 2006, approximately 0.14% of the non-federal lands in Puget

Sound were converted to a developed class each year. An independent Landsat-based study using data from 1986–2007 showed an annual rate of 0.5% of the land area changing to an urbanized class [55] while a US Forest Service study using 45,000 photo interpreted sample points, ranging from 1976 to 2006, found an annual new development rate of 0.38% [56]. Because land-use change in our study area over short time periods is spatially a rare event, typically acceptable land cover map accuracy rates of ~85% may be inadequate to effectively measure land cover change [57]. For example, an 85% correct map of change in an area with a real change rate of 1% would overestimate change by over an order of magnitude [58].

2.2. Image Data Processing

High resolution aerial imagery (1 m) from the U.S. National Agriculture Imagery Program (NAIP) was used as the primary data source. These data are being widely explored for their use in providing land-cover/land-use and change detection information [59–63]. Washington has complete state NAIP data for 2006, 2009, 2011, and 2013. Georectified NAIP image data were acquired from the WA Department of Natural Resources in 10 km × 10 km tiles. Whole watershed mosaics were created for the two time periods each with 68,144 rows and 90,392 columns of pixels (Figure 3). The 2006 data had three visible spectral bands and was delivered at an 18-inch resolution. The 2006 data was resampled in ERDAS Imagine to one meter to match the resolution of the 2009 data. Additionally, the 2009 data included a fourth band covering the near infra-red spectrum. A three-band difference image was generated by subtracting the 2006 three-band data from the three visible bands of the 2009 data.

For the 2009 data, the Normalized Difference Vegetation Index (NDVI) was calculated using the red and near infra-red bands according to [64]:

$$\frac{NIR - red}{NIR + red} \quad (1)$$

A 9 × 9 pixel simple-variance layer was calculated for the infra-red band as a measure of texture [65]. These two layers were added to the four-band 2009 image to create a six-layer data stack for 2009.

We created a land cover raster from the 2009 imagery to use the proportional area of different land cover types in each segment as input to the statistical model for predicting change. Only the 2009 imagery was used to generate land cover since the 2006 imagery lacked the NIR band and the ability to generate an NDVI image. The vegetation/no-vegetation mask created from the NDVI image was used to split the image into vegetated and non-vegetated images [65,66]. These two images were separately subjected to unsupervised classification. Twenty-five spectral classes were generated for the non-vegetation image and 50 for the vegetation image. The classes in these two resulting layers were aggregated separately and then added back together to create a 2009 land cover classification. The non-vegetation image was aggregated into the following classes: (1) shadow/water; (2) built/gray; (3) bare ground; and (4) uncertain. The vegetation fraction was classified as (5) herb/grass; (6) tree; and (7) shrub/indeterminate. Since the land cover classification was only used to inform the change model, a shadow class was used to recognize the inability to discern actual classes from limited reflected energy [67]. The shrub class was considered a semi-indeterminate class as the difference between dark grass, shrubs, and brightly lit trees can be very hard to distinguish [68–70].

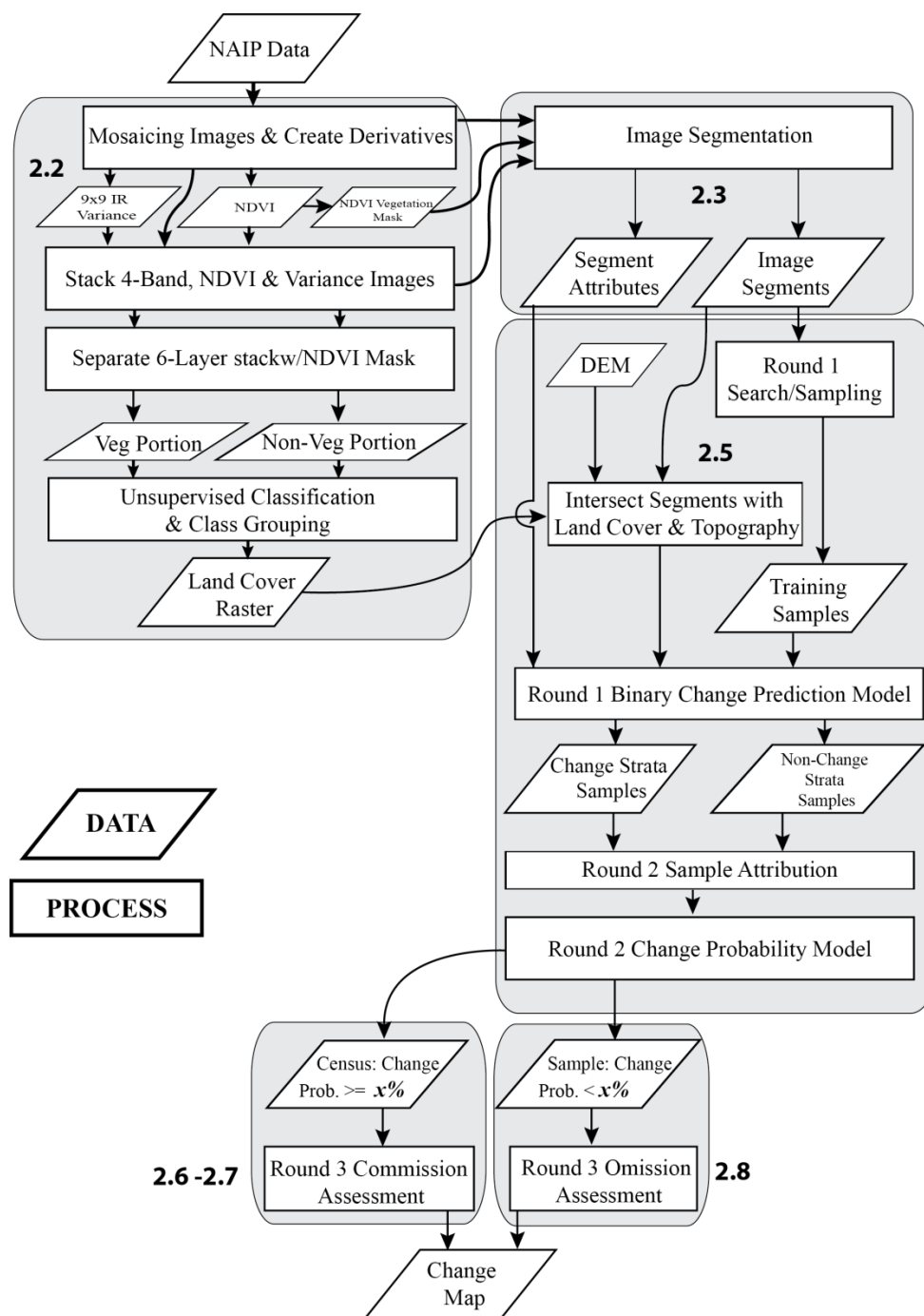


Figure 3. Flowchart of overall change mapping methodology. Shaded boxes represent sections within the methods with the section number bolded. The x represents the change threshold.

2.3. Segment Generation

Object-based image analysis starts with image segmentation in which pixels are grouped into polygons representing homogenous regions in space [18,41]. The segmentation process was performed using eCognition 8.7 and the eCognition server [71]. The process of segmentation with eCognition involves writing rule-sets that can incorporate multiple segmentation algorithms and hierarchical relationships and can weigh different image layers and complexity criteria to create objects

representing the users intended goals [27]. For this analysis, the primary goal was for changed locations to result in generating separate polygons. The 13 image layers involved in the segmentation process, were the three 2006 bands, the six-layer stack from 2009, the three difference bands and a vegetation/non-vegetation mask derived from the 2009 NDVI layer. For the NDVI-based mask, positive values were mapped as vegetated and values of zero or less were mapped as non-vegetation. Because we were interested in mapping changes specifically, the segmentation was performed simultaneously across time periods. The segmentation process proceeded from large landscape features, down to progressively smaller pieces and then segments with minimal absolute value in the difference layers were coalesced leading to the final analysis set. By performing the segmentation simultaneously across the change interval, the analysis was better able to focus on delineating changed areas as separate polygons and minimized the production of sliver polygons due to random image differences [72]. The polygons were exported as a simple feature with attributes derived from eCognition (Table 1). This is an iterative procedure and particular to the specific available data sets, so a detailed explanation of the rule-set used is not included. Segments ranged in size from less than a 1/10 ha in heterogeneous areas up to around 50 ha in places like continuous forested zones and large water bodies. The final segment layer is a complete polygon map of the original image data with the intention that likely change areas are partitioned into their own polygons.

Table 1. Predictor variables for the Random Forests model. Predictors 1–41 were generated directly by eCognition [71]. These variables are the means or standard deviations of the pixel values comprising the image segment. Land cover proportions were derived from extracting per segment information from the 2009 Land Cover model. Elevation was derived from sampling a 10-m digital elevation model with the segments. Texture was assessed by gray-level co-occurrence matrix, GLCM [73]. Predictors 50–59 were derived from an exported data set of linked sub-objects generated as part of the segmentation process.

#	Polygon Attributes	Type/Units
1–3	2006 Bands: Red, Green, Blue	Polygon Mean
4–6	2009 Bands: Red, Green, Blue	Polygon Mean
7	2009 Band 4: Infrared	Polygon Mean
8	2009 Derived: NDVI	Polygon Mean
9–11	2009–2006 Difference: Red, Green, Blue	Polygon Mean
12–22	Same as 1–11	Polygon St. Deviation
23	Contrast neighbor 2006 Red	Contrast across polygon border
24	Contrast neighbor 2009 Red	Contrast across polygon border
25–26	2006, 2009 Average Visible Brightness	Polygon Mean
27	Brightness Difference	Polygon Mean
28–29	2006, 2009 Average Visible Saturation (gray level)	Polygon Mean
30	Difference in Saturation	Polygon Mean
31	Rectangular Fit	Shape Statistic
32	Edge to Area Ratio	Shape Statistic
33	Width of Main Branch	Meters
34–35	UTM Longitude, Latitude	Meters
36–37	2006, 2009 GLCM Homogeneity Red Band	Polygon Texture
38	GLCM Homogeneity Red Difference	Polygon Texture

Table 1. Cont.

#	Polygon Attributes	Type/Units
39–40	2006, 2009 GLCM Entropy Red Band	Polygon Texture
41	GLCM Entropy Red Diff	Polygon Texture
42–48	2009 Land Cover Proportions	Classification as Polygon % by class
49	Elevation	Polygon Mean (m)
50	Count of SubObjects	Statistic based on sub-objects
51	Variance of Saturation 06	Statistic based on sub-objects
52	Variance of Saturation 09	Statistic based on sub-objects
53	Variance of Saturation Difference	Statistic based on sub-objects
54	Variance of Brightness 06	Statistic based on sub-objects
55	Variance of Brightness 09	Statistic based on sub-objects
56	Variance of Brightness Difference	Statistic based on sub-objects
57	Variance of Edge-Area ratio	Statistic based on sub-objects
58	Variance of GLCM 2006 Red	Statistic based on sub-objects
59	Variance of GLCM 2009 Red	Statistic based on sub-objects

2.4. The AAClipGenerator and AAViewer Software System

We developed an accuracy assessment system that consisted of two programs designed to facilitate rapid review of polygons or polygon pairs for classification. The task of reviewing candidate polygons during training data generation and during accuracy assessment can be some of the most time consuming requirements of change detection projects [74]. The purpose of the accuracy assessment system was to extract as much of the processing time involved with image pair review into an automated step, which prepares for an efficient classification step.

The first program called the AAClipGenerator, written in C# and ArcObjects with ArcGIS 10.0 [75] and dependent on an ArcGIS MXD file, creates medium sized jpegs for each image representing a single polygon and its surrounding landscape. The scaling is such that the polygon of interest takes up about the middle third of the image. One jpeg is generated for each image layer with the outline of the polygon of interest such that three jpegs are created for each polygon: the before image (2006), the visible bands from the after image (2009) and the difference image. Single polygons do not necessarily represent entire change locations. These image files and their metadata file are the input for the second program.

The second program, the AAViewer, includes a simple user interface designed to minimize key strokes and the amount of time waiting for images to load, scrolling around multiple tables and inputting data into clicked fields while maximizing the proportion of analyst time spent attributing the target polygon. This program provides a simultaneous view of the images and a data entry pane for classifying them (Figure 4). Using this system, an analyst can routinely review and attribute 250–300 polygon triplets an hour. An additional benefit of this system is the ability to reproduce the decision environment for the analyst portion of the project. Since the images and viewer are self-contained, they can be easily passed to a second observer to repeat the analysis and archived with the project to allow future review of the decisions made under identical conditions regarding image scale and orientation. Our accuracy optimization techniques were made feasible largely due to the efficiency gained by this

set of programs. While currently still under development, the current working system can be obtained from the author.

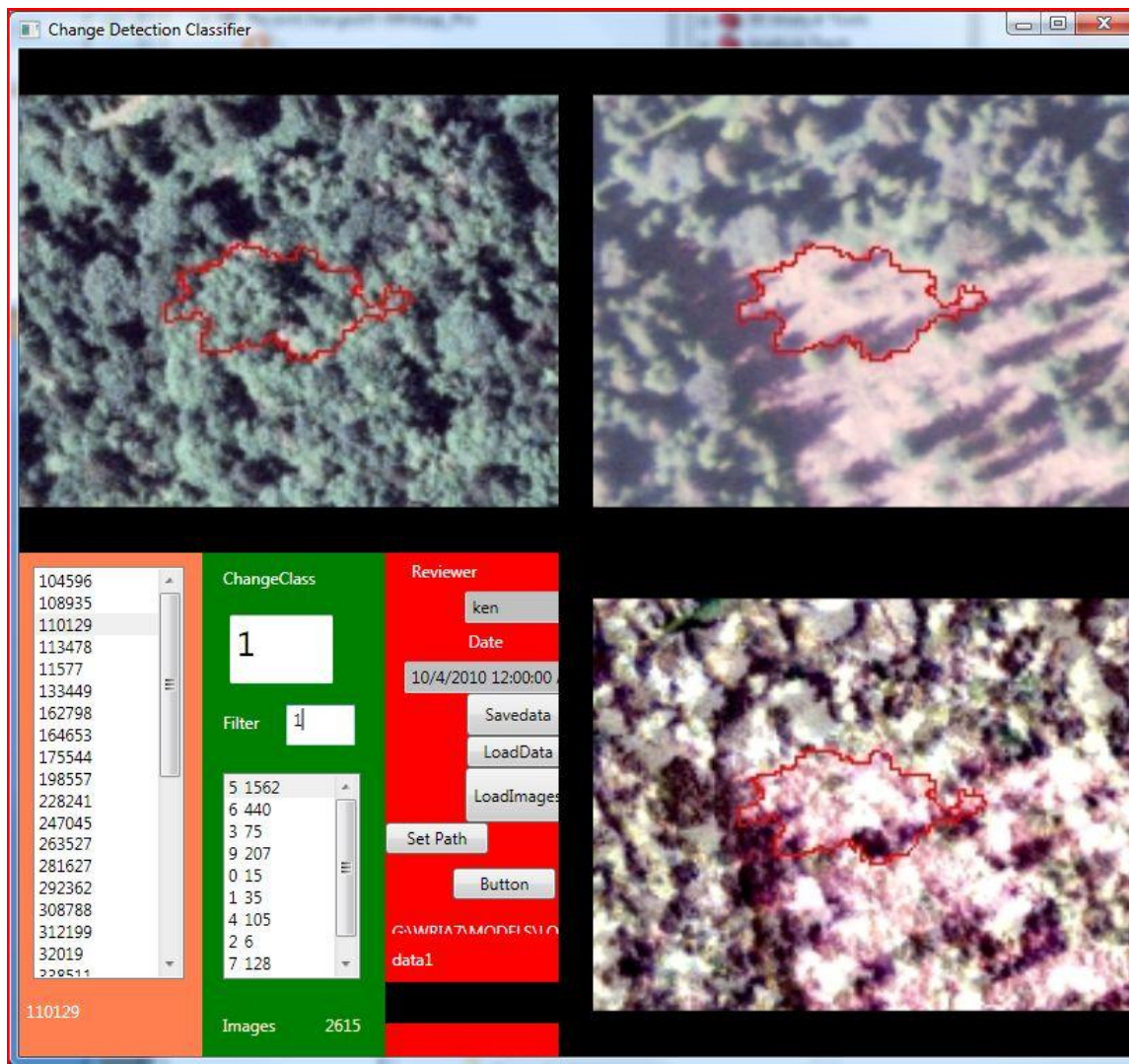


Figure 4. AAViewer. The AAViewer program displays three images and an attribution pane for rapidly classifying target polygons. In the figure, the upper left image is from 2006, the upper right image is from 2009, and the lower right image is the band-wise difference image. The ChangeClass box stays selected during review and movement between image sets is done with the “W” and “S” keys. The classification procedure requires 2 keystrokes, “S” to advance image sets and 1–9 to denote the change type.

2.5. Statistical Modeling with Random Forests

The segments (hereafter polygons) were used as the unit of analysis for the statistical model. Since land-cover change is a relatively rare event, we needed to stratify our sample to balance for our two classes, change and no change [52]. To achieve a balanced training sample we did two modeling iterations. To create the training data for the first iteration, we randomly selected ~500 polygons and manually searched for several hundred additional polygons that exhibited change-like differences in the imagery. While most of the change-like selected polygons were actual change (Figure 5A–E), we

included some polygons that looked like change but were actually only different due to view angle or illumination angle (Figure 5F), which are common problems for OBIA with high resolution imagery [15].

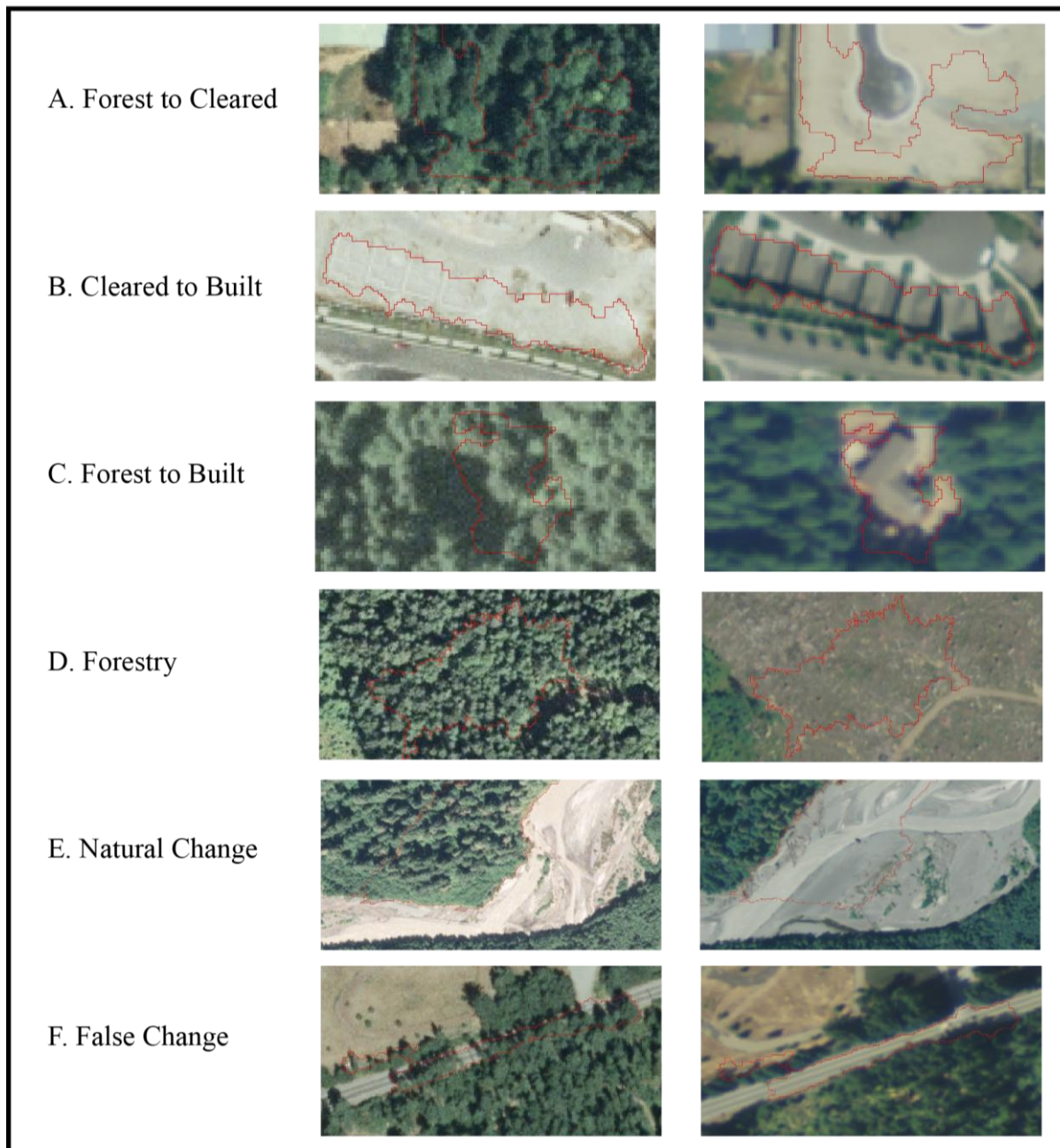


Figure 5. Examples of typical changes included in the training data. Changes like (A–C) were labeled as development in the final maps. Changes like (D) were labeled forestry. (E) Natural changes most commonly are stream course changes, land-slides and fires. (F) False changes are due to events like tree lean and shifting shadow patterns.

These initial polygons were labeled as either change-like, or not-change and used as the response in a Random Forest (RF) model [53,76–78] implemented with the randomForest package in the R statistical environment [79,80]. The predictor variables were derived from eCognition and ancillary

information derived from the land-cover modeling and topographic information (Table 1). Random Forests is a machine learning algorithm derived from Classification and Regression Trees (CART) [81,82]. CART is a recursive partitioning algorithm that searches a parameter space for a variable value that splits a data set into two leaves with the minimum possible classification error. It continues to split the leaves of the tree until some stopping rule such as “terminal leaf node variance dropping below some maximum value” is reached. Random Forests performs multiple iterations of a CART-style algorithm. For each tree it subsamples both the data and the predictor variable set. The final classification is essentially a voting scheme where each classification tree makes a prediction for each analysis unit and the final class is the class with the most votes. A probability is generated by observing the proportion of votes for the winning class *versus* the total number of trees. Because of this, interpreting RF results can be difficult if the analytical goal is to develop a mechanistic model for change. Relative importance is attributed to different variables depending on their cumulative contribution over the individual model runs.

From the initial model output, we randomly selected 2500 polygons from each strata, where the strata were the non-change and change-like predictions from the first iteration. These 5000 total samples were reviewed with the AAVIEWER and labeled as actual change or no-change. They were then used in the second modeling iteration as the response to create the final model. Based on the RF voting scheme, a change polygon is any polygon that was predicted to be change in the majority of derived classification trees or rather had a change probability of $\geq 50\%$. This produces the base output map which will be called the RF50 map, denoting the predicted change polygons from the model with a 50% change probability threshold.

2.6. Accuracy Optimization Technique 1—Eliminating Commission

All commission errors in the RF50 map are located among the polygons labeled as change, and all omission errors are among the polygons labeled as no-change. Therefore, to eliminate commission errors, an analyst used the AAVIEWER to observe and interpret each location predicted to be change based on our 50% minimum probability threshold denoted by the RF50 map, producing the new accuracy optimized AO50 map. Assuming half the model error was commission error, correcting all commission polygons should eliminate half of the model error. However, since change is rare, the number of polygons labeled as change is generally much smaller than those labeled as no-change, so the task of eliminating commission error is much smaller than trying to eliminate omission error.

This approach to error reduction was a hybrid method of regular predictive statistical modeling and analyst driven photo interpretation. The statistical modeling phase was used to focus the analyst's effort on those areas most likely to exhibit the target change events. In this way, predicted change areas were interpreted by an analyst and all mapped change polygons were effectively derived from photo interpretation [60,83]. We refer to this as an optimization because it goes beyond simply assessing the commission errors in the model and actually corrects them by removing them from the map.

2.7. Accuracy Optimization Technique 2—Lowering the Change Candidate Threshold

Our second enhancement to object-based change detection was a logical follow up to reviewing all potential change polygons. Eliminating commission errors allowed us to lower the minimum

probability threshold for accepting a polygon as a change candidate without inflating commission errors. While a series of thresholds could be used, we lowered the threshold to 25% to create the RF25 map and for comparison with the base RF50 map. The RF25 map was then submitted to our commission error assessment procedure to create the accuracy optimized AO25 map.

2.8. Estimating Omission

While pushing as much error into the commission fraction as possible, there will remain a small number of changes which, for whatever reason, conform poorly to the samples observed or which are simply computationally indistinguishable with the suite of predictor variables from locations that did not change. To estimate omission error from the remaining polygons, we reviewed a large sample (greater of 1% or 5000 polygons), for omission errors using the AAviewer. We calculated an areal-based omission rate where the rate is the proportion of area in the misclassified polygons divided by the total area observed in the omission sample [58]. This is similar to the prevalence weighting scheme used by Olofsson *et al.* (2013) [58] to calculate accuracy rates. The estimated omission area (O) is the product of the sum of the areas of the non-observed polygons (p_n) and the ratio of the sum of the areas of the changed omission polygons (p_c) divided by the sum of the areas of the observed omission polygons (p_o) [36,58]:

$$O = \sum p_n * \frac{\sum p_c}{\sum p_o} \quad (2)$$

A mapped change area and an estimated omission area were derived at the conclusion of the accuracy optimization process. The overall summary statistic for the analysis is the Adjusted Producer's Accuracy (APA), which is the ratio of the sum of the areas of the mapped change polygons (p_m) divided by the total predicted change area, which is the sum of the mapped change area plus the estimated omission area from Equation (2).

$$APA = \frac{\sum p_m}{\sum p_m + O} \quad (3)$$

An analogous Adjusted User's Accuracy could be calculated, but it is theoretically set to 100% by manually verifying all modeled change polygons.

2.9. Assessment of Accuracy Optimization

Accuracy optimization implies a balancing of effort with return. The primary optimization parameter in our proposed technique is the choice of change probability threshold. The combination of the commission and omission assessments provides information about error rates across the full spectrum of change probabilities and can provide a measure of the utility of assessing different change probability thresholds. To assess these we assigned all of the reviewed polygons, those from the commission and omission assessments, into 5% probability bins. The polygons in the bins with probability $\geq 25\%$ constituted a complete census as we reviewed every polygon of that sort. The polygons from the bins with $< 25\%$ probability were samples from the much larger population of lower change probability polygons. For each bin we plotted the observed percentage of reviewed polygons

that were actually change polygons against the median modeled probability for that bin. This provided a graphical representation of changing commission and omission rates by change probability. To assess an actual utility of reviewing different bins, a value must be assigned for finding additional change that can be weighed against analyst effort [84]. We will not assign a value at this time, but the framework to quantitatively assess a threshold is discussed.

3. Results

3.1. Comparison of Four Different Change Outputs

After conducting two accuracy optimization techniques, we had four versions of the change map: (a) a default output from the random forests model with a 50% map acceptance threshold (RF50); (b) the default random forests model with a 25% acceptance threshold (RF25); and the (c) AO50 and (d) AO25 maps, which are accuracy optimized version of the RF50 and RF25 maps, respectively, which result from removing commission error. Here, we will compare the overall mapped change area and commission error that resulted from applying these techniques.

Table 2. Overall summary of the two change models before and after commission removal. The table shows the number of polygons reviewed for each model, the area covered by those polygons, the area of commission errors removed, the final mapped change area and the count of change locations. Note that the AO25 map almost doubled the number of change locations. Change locations were derived from aggregating adjacent change polygons.

Model	Change Probability Threshold	Reviewed Change Polygons	Modeled Change Area (ha)	Removed Commission Area (ha)	Verified Change Area (ha)	Dissolved Change Locations
RF50/AO50 Map	≥50%	7832	3866	87	3779	2348
RF25/AO25 Map	≥25%	16,524	5354	833	4521	5607

3.2. Random Forests Statistical Prediction of Land Cover Change in the Puyallup Watershed, 2006–2009

The output from the random forest model comprised the base RF50 map from which we will make comparisons. The base RF50 map contained 7832 polygons out of the total population of 460,561. The size of these polygons ranged from 0.01 to 14.9 ha with an interquartile range of 0.13 to 0.54 ha. Of those change polygons, 878 were larger than 1 ha in size and collectively covered 48.8% of the change area. Based on area, the RF50 model-based annual change rate averaged 0.47%/year over the three year period.

3.3. Commission Error Removal from the RF50 Land Cover Change Map

To create the AO50 map we applied our commission removal technique to the RF50 map by reviewing all of the RF50 change polygons using the AAviwer. Of the 7832 change polygons, 472 covering an area of 87 ha were found to be erroneously classified as change, giving a commission error rate of 2.55% by area (Table 2). The resulting AO50 change map contained 3779 ha of change for a slightly reduced average annual change rate of 0.46%. Because of the relatively low commission error

rate, the overall change rate statistics changed little between the RF50 map and AO50 map. The total area reviewed for the AO50 map represented about 1.5% of the study area, which showed that eliminating commission error from the RF50 map, the base model output, required reviewing only 1/67th of the total study area. We used this fraction as an estimate of efficiency as compared to all manual photo interpretation.

While reviewing change polygons using the AAViewer, we attributed each to one of three change agents: development, forestry or natural. After removing commission errors, The AO50 map included 330 ha of development, 3002 ha of forestry, and 433 ha of natural related change. The average size of the forestry change polygons (5.43 ha) was considerably larger than the average size for development (0.37 ha) or natural changes (0.49 ha). Thus, the review process provided two benefits (1) the elimination of commission error and (2) an opportunity to designate a change agent.

3.4. Omission Estimate for the RF50/AO50 Change Model

Omission estimates associated with the RF50 map and AO50 map were identical because each model contained the same polygons labeled as no-change by the Random Forests model, those with change probabilities <50%. A random sample of 5346 no-change polygons, covering 3060 ha, was reviewed for this procedure using the AAViewer. Of those polygons, 95 contained change areas covering 13.6 ha resulting in an omission rate of 0.45% (change area/no-change area), which translated into an estimated 1172 ha of estimated omitted change ($0.0045 \times \text{total no-change area}$). A complete assessment of the initial RF50 model consisted of an actual commission error rate of 2.55% and an estimated omission error rate of 0.45%. The Adjusted Producer's Accuracy (APA) was calculated (Equation (3)) as 76.3% (3779 ha mapped plus 1172 ha additional predicted). This analysis also raised the percentage of total area observed to 2.6% (1/38th) of the study region.



Figure 6. Sample area showing the distribution of AO50 (blue) and AO25 (purple) change locations. AO50 locations were part of the base map. AO25 locations were mapped during the application of accuracy optimization technique 2. The area shown represents about 1% of the mapped watershed. With a scale of 1:20,000 the smallest mapped change locations (about 200 m²) represent about 8 pixels in the original figure.

3.5. Commission Error Removal from the RF25 Land Cover Change Map

When the change acceptance threshold was lowered from 50% to 25%, the new RF25 map consisted of 16,524 polygons labeled as change (Table 2), more than doubling the number from the RF50 map. The commission rate among the additional 25%–50% change probability polygons was much higher at 49.8% than the 2.55% rate for the >50% polygons. Combined, the overall commission rate for the RF25 map was 15.6%. The additional polygons added 742 ha of change. Those new change polygons consisted of 322 ha of development, 268 ha of forestry and 161 ha of natural change. The increase in area for the three types of change was 96%, 9% and 38%. Note that while little forestry related change was missed in the AO50 map, almost half of the mapped development related change was missed (Figure 6). Additionally the number of verified unique change locations increased by 238% between the AO50 and AO25 maps (Table 2).

3.6. Omission Estimate for the RF25/AO25 Change Map

All polygons with change probabilities of 25%–50% switched from no-change polygons to candidate change polygons in the RF25 map. This altered the population of no-change polygons from which the omission sample was drawn. Of the original 5346 polygons in the RF50 omission sample, only 96 had a reassignment from no-change to change in the RF25 analysis. While the change threshold was cut in half, only 1.8% of the polygons from the original omission sample were relabeled. The distribution of polygons by change probability was heavily skewed towards low probabilities with 74.5% of all polygons having lower than a 5% probability of being change (Figure 7) and, thus, most of the random sample to estimate omission came from these low probability bins. However, the 1.8% that did switch accounted for 39% of the previously identified omission errors and was remapped as change in the RF25 and subsequent AO25 maps. The remaining 58 omission polygons previously assessed as change had an area of 8.2 ha which included 5.6 ha (68%) of development, 1.5 ha (18%) of forestry and 1.1 ha (14%) of natural change.

The size distribution of the missed change polygons was different from the overall distribution of polygon sizes. The average omitted change polygon was 0.14 ha compared to the overall average polygon checked for omission that was 0.58 ha. Therefore the estimated missed change was the ratio of observed change area in the Omission sample divided by the overall area of the Omission sample (Equation (2)). Only 8.2 ha of omitted change were found among 3046 ha of observations lowering the omission rate from 0.45% to 0.27%. This rate was multiplied by the remaining area of predicted non-change for a total omission estimate of 701 ha. This also raised the total estimated change to 5222 ha with a mapped change area of 4521 ha. The final APA was 86.6% ($4521 \text{ ha} / (4,521 \text{ ha} + 701 \text{ ha})$). A simple areal accuracy rate for the final change map was 99.73% which assumes only the predicted 701 ha of omission error was incorrectly mapped. That also yielded a final annual change rate of 0.55% or a cumulative change of 1.66% for the three year period.

3.7. Accuracy Optimization Assessment

The primary trade-off to consider when setting a minimum change probability threshold is whether the increased change mapping is commensurate with the increased time to review additional candidate

change polygons. We plotted the observed change proportion in 5% probability bins over the bin median predicted probability of change (Figure 7). The proportion of polygons observed as change had a sigmoidal relationship with increasing probability. For the lowest bin, 0%–5%, only 0.2% of observed sample polygons were actual change while, in the highest bin, 95%–100%, 100% were actually change.

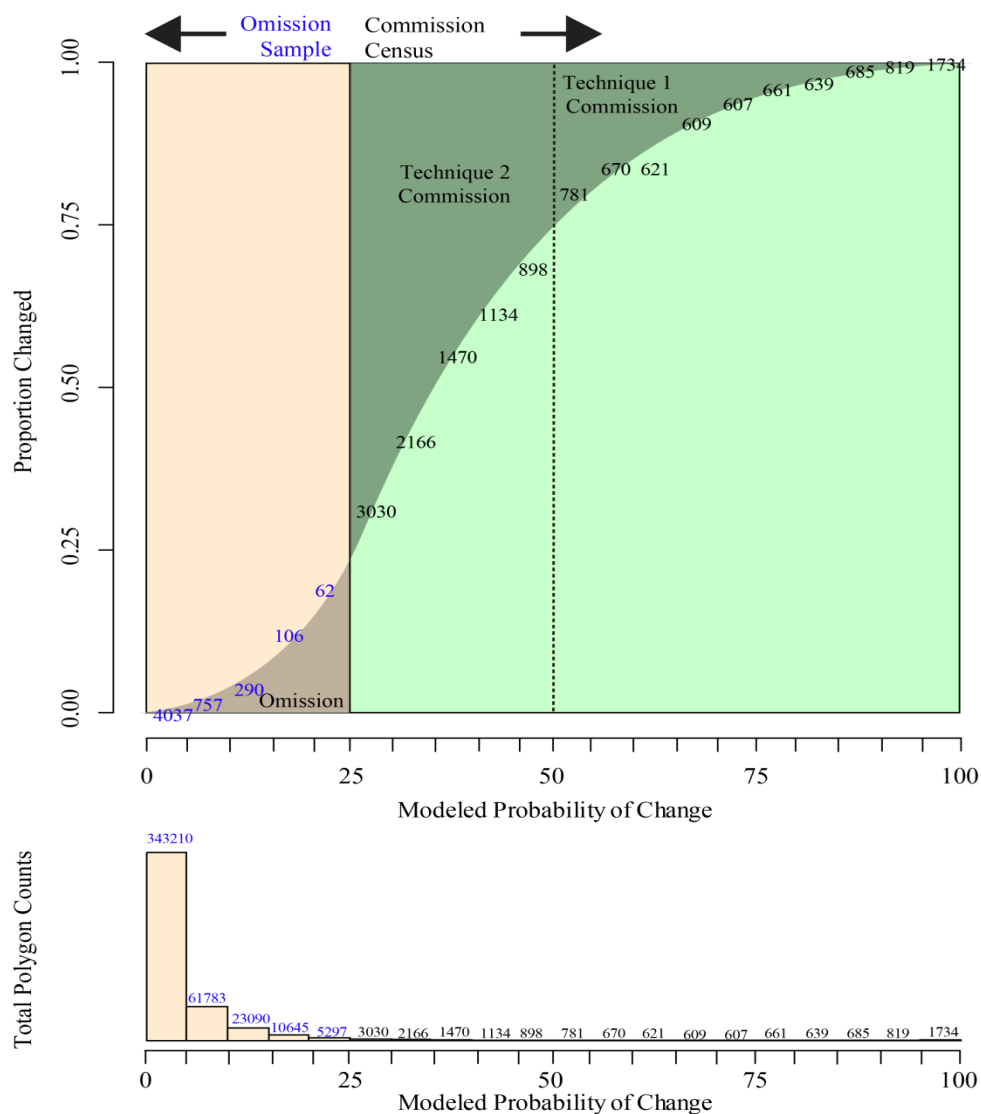


Figure 7. Plots of observed change proportion and polygon counts by 5% probability bins. The upper plot shows the number of observed polygons in each bin plotted on the y-axis as the percentage of observed change polygons for that bin. For example, the uppermost value of 1734 represents the 95%–100% probability bin for reviewed polygons which contained 1734 polygons of which all were actually change. Values to the right of 25% are complete censuses. Values to the left of 25% represent proportionate samples with change probabilities <25%. The darker areas represent errors of commission and omission. The light green area between 25 and 50% provides a graphical representation of additional change mapped from accuracy optimization technique 2, threshold lowering. The bottom histogram shows the total population of polygons in each bin.

The lowest 5 bins, which were assessed during the omission analysis, had rates from 0.2% to 19% (Table 3). We used these percentages to estimate the cost of reviewing subsequent bins. To estimate utility we would need to assign a value on mapping additional change and compare it to our estimated cost [84]. For example, the 10%–15% bin had 23,090 polygons in it from which we observed a sample of 290 polygons. Those polygons covered 69 hectares of which we observed 1.3 were omitted change. If we extend the proportion of change in this bin, 1.89%, by the 5754 acres covered by all polygons in this bin, we might expect to find 108 total change hectares if we performed the census. The cost to map these additional change locations would be about 92 hours of analyst time.

Table 3. Omission analysis extent, effort, observations and predictions for different predicted change probabilities in sample-only bins. The observed polygons consisted of the Omission samples. Columns show the areal extent and polygon count for each bin, the polygons observed and the number of polygons observed as omitted change. The last three columns in italics are predictions based on observed proportions. Predictions can be made by using either the proportion of observed polygons that changed or the proportion of area observed that changed. Review hours are based on a rate of 250 polygons per hour.

Bins	Polygons	Hectares	Observed Polygons	Observed Hectares	Observed Change Polygons	Observed Change Hectares	Polygon Percent Change	Area Percent Change	Polygon Prediction	Hectares Prediction	Hours To Review
(0%–5%)	343210	237400	4037	2705	9	1.1	0.2%	0.04%	<i>765</i>	<i>94</i>	<i>1373</i>
(5%–10%)	61783	15708	757	193	12	1.3	1.6%	0.68%	<i>979</i>	<i>107</i>	<i>247</i>
(10%–15%)	23090	5754	290	69	12	1.3	4.1%	1.89%	<i>955</i>	<i>108</i>	<i>92</i>
(15%–20%)	10645	2906	106	26	13	2.8	12.3%	11.10%	<i>1306</i>	<i>322</i>	<i>43</i>
(20%–25%)	5297	968	62	8	12	1.6	19.4%	21.50%	<i>1025</i>	<i>208</i>	<i>21</i>

The review of the 5734 training polygons for input to the Random Forests model took about 24 hours. The workload for the Commission analysis is proportional to the number of polygons in each prediction bin. The perceived value for reviewing a certain prediction bin is proportional to the change rate observed in that bin. The RF50 accuracy assessment required the review of 7832 polygons for commission errors and 5250 polygons for omission errors which totaled 13,108 polygons and required 50–60 analyst hours. The additional polygons for the RF25 analysis raised the accuracy assessment work load to 21,774 polygons, added 40 hours of processing and raised the number of mapped change locations from 2348 to 5607.

4. Discussion

The goal for this work was to find an optimal method for mapping land-cover change that could approach the high level of accuracy achieved through manual photo-interpretation but conducted at regional extents that usually necessitate an automated remote sensing approach. The threshold setting task in our process provides the optimization between these two approaches. At a threshold of 100%, no polygons would be reviewed and the result is the RF50 map, an entirely automated approach. If the threshold is set at 0%, all polygons would be reviewed and the result would be a photo-interpreted

map. At 25%, we observed roughly 4.7% of the total population of polygons with an estimated success rate of 86.6% as measured by the Adjusted Producer's Accuracy.

4.1. Improved Map Accuracy for Data Integration

To answer questions of public interest such as those pertaining to natural resource management and land-use planning effectiveness, regional and local governments need to be able to integrate land-use/land-cover change (LULCC) data with other GIS data sources. This requires LULCC data with high spatial resolution and spatial precision because many such data sources have individual units that cover relatively small areas in relation to a medium resolution, 30-m pixel [61]. For example, changes in regulated riparian corridors [59], urban infilling and new satellite development within undisturbed canopies [85] frequently occur at scales smaller than the Landsat minimum mapping unit. To address these needs, object-based change detection methods were used with 1-m publicly available aerial imagery.

By lowering the acceptance threshold from 50% in RF50 to 25% in the RF25 map, 93% more development-related change was detected. Further, while, the initial RF50 map captured 85% of the total mapped change area, the RF25 data was heavily skewed towards identifying small permanent changes, *i.e.*, average size of >50%-probability changes was 0.51 ha compared to 25%–50%-probability changes that had an average size of 0.19 ha. Not surprisingly, bigger changes are easier to detect. By type, the average Forestry polygon was 5.43 ha (1275 locations) compared to 0.42 ha for Natural change (2001 locations) and 0.37 ha for Development change (2252 locations). Locating development-related changes was the highest priority because changes associated with human development (urbanization) while usually small, are mostly permanent and often inform how well local governments are meeting their responsibilities under land use planning laws, such as the WA State Growth Management Act (GMA, Chapter 36.70A RCW) or the Shoreline Management Act (SMA, Chapter 90.58 RCW).

For example, Jensen [86] used high-resolution change location data in an analysis of conservation effectiveness in the Cedar-Sammamish watershed in the Puget Sound region of Washington. Jensen located 72 change events between 2006 and 2009 occurring adjacent to streams, totaling 18.7 ha. The cause of change was determined for each change location and evaluated relative to ownership and land-use category. Natural change was the most common change type (7.8 ha) followed by development (5.5 ha) and transportation projects (4.1 ha). Importantly, no change was mapped on parcels containing conservation easements or other land use restrictions suggesting these conservation mechanisms were adequately protecting riparian buffers.

The final change map consisted of 1.66% change and 98.34% no-change. Thus, if an uninformative model had been used and simply mapped no change, the overall accuracy would have still been 98.34%. However the commission analysis discovered a 2.55% commission error rate for the base map polygons and a 49.8% commission rate for the additional 25%–50% probability polygons. The omission analysis yielded a 0.27% error rate of omission. Since the commission was eliminated, the only error in the final map was the omission area and the final map overall accuracy was 99.73%, 1.39% better than mapping no change at all. Importantly, some of the common accuracy statistics also become uninformative after applying these procedures. For example, the User's Accuracy assesses the

probability that a location mapped as a certain class will be that class. By eliminating commission error the User's Accuracy for the final map was 100%. This informs the user that all mapped changes are actually changes. However, for practical usage, neither a producer's or user's accuracy of 100% nor an overall accuracy of 99.73% conveys much information about the success of the analysis. During the development of these techniques the proportion of mapped change relative to total predicted change was frequently used as a metric of success. This is roughly equivalent to Olofsson *et al.*'s [58] Adjusted Producer's Accuracy (APA). The APA statistic may be preferable because it describes the real quantity of interest; the amount and location of change. This analysis resulted in an estimation of overall change area for which the location is known for 86.6%. Thus, when asking questions about the data or when intersecting the change area with other data sets, the results are expected to capture on average a minimum of 86.6% of the overall change.

4.2. The AAClipGenerator/AAViewer System

The AAViewer system can also be used by other analysts to improve their work because its use can eliminate commission errors and improve overall prediction accuracy for a given amount of effort. The AAViewer system was written to facilitate checking model results rapidly. The tool succeeded in drastically reducing the time necessary for the verification of model results leading to a complete census of predictions and thus the elimination of commission errors. The AAViewer tool can be similarly applied by others to improve the efficiency and accuracy of their LULCC projects.

Criteria should be developed for deciding when the tradeoff between additional effort and increased accuracy is optimal. At this point the balancing of tradeoffs is purely subjective and should be informed by the research question. Ideally, one would be able to assign a value to mapping each individual change event and compare it to the cost of an analyst's time to find that event and create a stopping rule when they are equal. At high change probabilities, an analyst may find every reviewed polygon is a change. At low probability frequencies, an analyst may need to review 10–20 polygons to find a single change event. As such, the cost to find additional change continues to increase as polygons with smaller change probabilities are reviewed.

5. Conclusions

Several aspects of this work may have important implications for future LULCC characterization for research and management applications. In brief:

1. The combined accuracy optimization techniques improved the detection of urbanizing land-cover by increasing the mapped development-related change area by 93% in the AO25 map compared to the base map produced by the initial prediction model, the RF50 map and raised the total number of individual mapped change locations by 239% from 2348 to 5607 (Table 2).
2. A total change estimate was generated by both "eliminating" commission and estimating omission. That estimate was comprised of 86.6% mapped change events and 13.4% estimated unmapped change.

3. A software system was developed to assess training data locations and to determine classification accuracy that greatly reduced analyst review time allowing review of 1000s of accuracy assessment and training data locations in the time previously required to view 100s.
4. Searching for additional change through threshold lowering is a powerful technique for optimizing change mapping when using a probabilistic classifier like RF and a system for rapidly checking predictions as developed here.
5. The image data used in this analysis is available for many parts of the United States and the techniques described here are applicable to any object-based mapping exercise using imagery of high enough resolution to verify classifications through manual photo interpretation.

Previous LULCC maps have tended to capture either big events over large regions using medium resolution data and remote sensing analyses or small-to-large events over small regions using high resolution data and photo interpretation. To achieve fine-scale change mapping over large extents remote sensing analyses were used to locate potential small-to-large events over large regions using high resolution data. Then photo interpretation was employed over the much smaller though widely dispersed candidate regions to complete mapping those changes. Thus, traditional remote sensing techniques were used to find locations for photo interpretation. Recreation of the full system does involve significant software resources including ESRI ArcMap, Erdas Imagine and Trimble eCognition [71,75,87]. For large regions (images greater than 10 k × 10 k pixels) the eCognition server software is highly recommended.

Acknowledgments

The author greatly appreciates the support and input of all members of our research team, especially Jeanne Miller and Kevin Samson. The author also acknowledges the invaluable review comments from Timothy Quinn, Kirk Krueger, Karis Tenneson, Andy Gray and three anonymous reviewers. This work was supported by an EPA LO-Watershed Grant PC00-J27601-4. Product or company names mentioned in this publication are for the reader information only and do not imply endorsement by the Washington Department of Fish and Wildlife of any product or service.

Conflicts of Interest

The author declares no conflict of interest.

References and Notes

1. Rindfuss, R.R.; Walsh, S.J.; Turner, B.L.; Fox, J.; Mishra, V. Developing a science of land change: Challenges and methodological issues. *Proc. Natl. Acad. Sci. USA* **2004**, *101*, 13976–13981.
2. Turner, B.; Lambin, E.F.; Reenberg, A. The emergence of land change science for global environmental change and sustainability. *Proc. Natl. Acad. Sci. USA* **2007**, *104*, 20666–20671.
3. Solecki, W.; Seto, K.C.; Marcotullio, P.J. It's Time for an Urbanization Science. *Environ. Sci. Policy Sustain. Dev.* **2013**, *55*, 12–17.
4. Rogan, J.; Chen, D. Remote sensing technology for mapping and monitoring land-cover and land-use change. *Prog. Plann.* **2004**, *61*, 301–325.

5. Kennedy, R.E.; Townsend, P.A.; Gross, J.E.; Cohen, W.B.; Bolstad, P.; Wang, Y.Q.; Adams, P. Remote sensing change detection tools for natural resource managers: Understanding concepts and tradeoffs in the design of landscape monitoring projects. *Remote Sens. Environ.* **2009**, *113*, 1382–1396.
6. Petter, M.; Mooney, S.; Maynard, S.M.; Davidson, A.; Cox, M.; Horosak, I. A methodology to map ecosystem functions to support ecosystem services assessments. *Ecol. Soc.* **2013**, *18*, 31.
7. Thackway, R.; Lymburner, L.; Guerschman, J.P. Dynamic land cover information: Bridging the gap between remote sensing and natural resource management. *Ecol. Soc.* **2013**, *18*, doi:10.5751/ES-05299-180102.
8. Goetz, S.J.; Wright, R.K.; Smith, A.J.; Zinecker, E.; Schaub, E. IKONOS imagery for resource management: Tree cover, impervious surfaces, and riparian buffer analyses in the mid-Atlantic region. *Remote Sens. Environ.* **2003**, *88*, 195–208.
9. Wulder, M.A.; Hall, R.J.; Coops, N.C.; Franklin, S.E. High Spatial Resolution Remotely Sensed Data for Ecosystem Characterization. *Bioscience* **2004**, *54*, 511–521.
10. Morgan, J.L.; Gergel, S.E.; Coops, N.C. Aerial photography: A rapidly evolving tool for ecological management. *Bioscience* **2010**, *60*, 47–59.
11. Lu, D.; Hetrick, S.; Moran, E. Impervious surface mapping with QuickBird imagery. *Int. J. Remote Sens.* **2011**, *32*, 2519–2533.
12. Johansen, K.; Roelfsema, C.; Phinn, S. SPECIAL FEATURE—High Spatial Resolution Remote Sensing for Environmental Monitoring and Management PREFACE: *J. Spat. Sci.* **2008**, *53*, 43–48.
13. Myint, S.W.; Gober, P.; Brazel, A.; Grossman-Clarke, S.; Weng, Q. Per-pixel vs. object-based classification of urban land cover extraction using high spatial resolution imagery. *Remote Sens. Environ.* **2011**, *115*, 1145–1161.
14. Baker, B.A.; Warner, T.A.; Conley, J.F.; Mcneil, B.E. Does spatial resolution matter? A multi-scale comparison of object-based and pixel-based methods for detecting change associated with gas well drilling operations. *Int. J. Remote Sens. Publ.* **2012**, *34*, 37–41.
15. Chen, G.; Hay, G.J.; Carvalho, L.M.T.; Wulder, M.A. Object-based Change Detection. *Int. J. Remote Sens.* **2012**, *33*, 4434–4457.
16. Desclée, B.; Bogaert, P.; Defourny, P. Forest change detection by statistical object-based method. *Remote Sens. Environ.* **2006**, *102*, 1–11.
17. Zhou, W.; Troy, A. An object-oriented approach for analysing and characterizing urban landscape at the parcel level. *Int. J. Remote Sens.* **2008**, *29*, 3119–3135.
18. Blaschke, T.; Lang, S.; Hay, G.J. *Object-Based Image Analysis: Spatial Concepts for Knowledge-Driven Remote Sensing Applications*; Lecture Notes in Geoinformation and Cartography; Springer-Verlag: Berlin/Heidelberg, Germany, 2008.
19. Morgan, Jessica, Gergel, S. Automated analysis of aerial photographs and potential for historic forest mapping. *Can. J. For. Res.* **2013**, *43*, 699–710.
20. Lillesand, T.; Kiefer, R.W.; Chipman, J. *Remote Sensing and Image Interpretation*; John Wiley Sons Inc.: New York, NY, USA, 2003.
21. Du, P.; Liu, P.; Xia, J.; Feng, L.; Liu, S.; Tan, K.; Cheng, L. Remote sensing image interpretation for urban environment analysis: methods, system and examples. *Remote Sens.* **2014**, *6*, 9458–9474.

22. Jelinski, D.E.; Wu, J. The modifiable areal unit problem and implications for landscape ecology. *Landscape Ecol.* **1996**, *11*, 129–140.
23. Linke, J.; McDermid, G.J.; Pape, A.D.; McLane, A.J.; Laskin, D.N.; Hall-Beyer, M.; Franklin, S.E. The influence of patch-delineation mismatches on multi-temporal landscape pattern analysis. *Landscape Ecol.* **2008**, *24*, 157–170.
24. Karl, J.W.; Maurer, B.A. Multivariate correlations between imagery and field measurements across scales: comparing pixel aggregation and image segmentation. *Landscape Ecol.* **2009**, *25*, 591–605.
25. Aubrecht, C.; Steinnocher, K.; Hollaus, M.; Wagner, W. Integrating earth observation and GIScience for high resolution spatial and functional modeling of urban land use. *Comput. Environ. Urban Syst.* **2009**, *33*, 15–25.
26. Johansen, K.; Phinn, S.; Witte, C. Mapping of riparian zone attributes using discrete return LiDAR, QuickBird and SPOT-5 imagery: Assessing accuracy and costs. *Remote Sens. Environ.* **2010**, *114*, 2679–2691.
27. O’Neil-Dunne, J.; MacFaden, S.; Royar, A. A versatile, production-oriented approach to high-resolution tree-canopy mapping in urban and suburban landscapes using GEOBIA and data fusion. *Remote Sens.* **2014**, *6*, 12837–12865.
28. Hong, B.; Limburg, K.E.; Hall, M.H.; Mountrakis, G.; Groffman, P.M.; Hyde, K.; Luo, L.; Kelly, V.R.; Myers, S.J. An integrated monitoring/modeling framework for assessing human–nature interactions in urbanizing watersheds: Wappinger and Onondaga Creek watersheds, New York, USA. *Environ. Model. Softw.* **2012**, *32*, 1–15.
29. Levin, S.A.; Dec, N. The problem of pattern and scale in ecology: The Robert H. MacArthur Award Lecture. *Ecology* **1992**, *73*, 1943–1967.
30. Wu, H.; Li, Z.-L. Scale issues in remote sensing: A review on analysis, processing and modeling. *Sensors* **2009**, *9*, 1768–1793.
31. Burnicki, A.C. Impact of error on landscape pattern analyses performed on land-cover change maps. *Landscape Ecol.* **2012**, *27*, 713–729.
32. Stehman, S. V.; Wickham, J.D. Assessing accuracy of net change derived from land cover maps. *Photogramm. Eng. Remote Sens.* **2006**, *72*, 175–185.
33. Walter, V. Object-based classification of remote sensing data for change detection. *ISPRS J. Photogramm. Remote Sens.* **2004**, *58*, 225–238.
34. Burnett, C.; Blaschke, T. A multi-scale segmentation/object relationship modelling methodology for landscape analysis. *Ecol. Model.* **2003**, *168*, 233–249.
35. Blaschke, T. Object based image analysis for remote sensing. *ISPRS J. Photogramm. Remote Sens.* **2010**, *65*, 2–16.
36. Congalton, R.G.; Green, K. *Assessing the Accuracy of Remotely Sensed Data: Principles and Practices, Second Edition (Mapping Science)*; CRC Press: Boca Raton, FL, USA, 2008.
37. Fawcett, T. An introduction to ROC analysis. *Pattern Recognit. Lett.* **2006**, *27*, 861–874.
38. Lu, D.; Weng, Q. A survey of image classification methods and techniques for improving classification performance. *Int. J. Remote Sens.* **2007**, *28*, 823–870.
39. Strahler, A.H.; Woodcock, C.E.; Smith, J. A. On the nature of models in remote sensing. *Remote Sens. Environ.* **1986**, *20*, 121–139.

40. Woodcock, C.E.; Strahler, A.H. The factor of scale in remote sensing. *Remote Sens. Environ.* **1987**, *21*, 311–332.
41. Haralick, R.M.; Shapiro, L.G. Image segmentation techniques. *Comput. Vis. Graph. Image Process.* **1985**, *29*, 100–132.
42. Hay, G.J.; Castilla, G.; Wulder, M.A.; Ruiz, J.R. An automated object-based approach for the multiscale image segmentation of forest scenes. *Int. J. Appl. Earth Obs. Geoinf.* **2005**, *7*, 339–359.
43. Lu, D.; Mausel, P.; Brondízio, E.; Moran, E. Change detection techniques. *Int. J. Remote Sens.* **2004**, *25*, 2365–2401.
44. Weng, Q. Remote sensing of impervious surfaces in the urban areas: Requirements, methods, and trends. *Remote Sens. Environ.* **2012**, *117*, 34–49.
45. Singh, A. Digital change detection techniques using remotely-sensed data. *Int. J. Remote Sens.* **1989**, *10*, 989–1003.
46. Coppin, P.; Jonckheere, I.; Nackaerts, K.; Muys, B.; Lambin, E. Digital change detection methods in ecosystem monitoring: A review. *Int. J. Remote Sens.* **2004**, *25*, 1565–1596.
47. Linke, J.; Mcdermid, G.J.; Laskin, D.N.; Mclane, A.J.; Pape, A.; Cranston, J.; Franklin, S.E. A disturbance-inventory framework for flexible and reliable landscape monitoring. *Photogramm. Eng. Remote Sens.* **2009**, *75*, 981–995.
48. Im, J.; Jensen, J.R.; Tullis, J.A. Object-based change detection using correlation image analysis and image segmentation. *Int. J. Remote Sens.* **2008**, *29*, 399–423.
49. Foody, G.M. Status of land cover classification accuracy assessment. *Remote Sens. Environ.* **2002**, *80*, 185–201.
50. Nusser, S.; Klaas, E. Survey methods for assessing land cover map accuracy. *Environ. Ecol. Stat.* **2003**, *10*, 309–331.
51. Edwards, T.; Moisen, G.; Cutler, D. Assessing map accuracy in a remotely sensed, ecoregion-scale cover map. *Remote Sens. Environ.* **1998**, *63*, 73–83.
52. Stehman, S.; Czaplewski, R. Design and analysis for thematic map accuracy assessment: Fundamental principles. *Remote Sens. Environ.* **1998**, *344*, 331–344.
53. Hastie, T.; Tibshirani, R.; Friedman, J. *The Elements of Statistical Learning: Data Mining, Inference, and Prediction, Second Edition (Springer Series in Statistics)*; Springer: New York, NY, USA, 2009.
54. Aleksandrowicz, S.; Turlej, K.; Lewiński, S.; Bochenek, Z. Change detection algorithm for the production of land cover change maps over the European Union countries. *Remote Sens.* **2014**, *6*, 5976–5994.
55. Hepinstall-Cymerman, J.; Coe, S.; Hutyra, L.R. Urban growth patterns and growth management boundaries in the Central Puget Sound, Washington, 1986–2007. *Urban Ecosyst.* **2013**, *16*, 109–129.
56. Gray, A.N.; Azuma, D.L.; Lettman, G.J.; Thompson, J.L.; McKay, N. *Changes in Land Use and Housing on Resource Lands in Washington State, 1976–2006*; USDA PNW Research Station: Washington, DC, USA, 2013.
57. Pontius, R.G.; Shusas, E.; McEachern, M. Detecting important categorical land changes while accounting for persistence. *Agric. Ecosyst. Environ.* **2004**, *101*, 251–268.

58. Olofsson, P.; Foody, G.M.; Stehman, S.V.; Woodcock, C.E. Making better use of accuracy data in land change studies: Estimating accuracy and area and quantifying uncertainty using stratified estimation. *Remote Sens. Environ.* **2013**, *129*, 122–131.
59. Liknes, G.; Perry, C.; Meneguzzo, D. Assessing tree cover in agricultural landscapes using high-resolution aerial imagery. *J. Terr. Obs.* **2010**, *2*, 38–55.
60. Claggett, P.R.; Okay, J. a.; Stehman, S.V. Monitoring regional Riparian forest cover change using stratified sampling and multiresolution imagery. *J. Am. Water Resour. Assoc.* **2010**, *46*, 334–343.
61. Moskal, L.M.; Styers, D.M.; Halabisky, M. Monitoring urban tree cover using object-based image analysis and public domain remotely sensed data. *Remote Sens.* **2011**, *3*, 2243–2262.
62. Li, X.; Shao, G. Object-based land-cover mapping with high resolution aerial photography at a county scale in midwestern USA. *Remote Sens.* **2014**, *6*, 11372–11390.
63. Yuan, F. Land cover change and environmental impact analysis in the Greater Mankato area of Minnesota using remote sensing and GIS modelling. *Int. J. Remote Sens.* **2008**, *29*, 1169–1184.
64. Goward, S.N.; Davis, P.E.; Fleming, D.; Miller, L.; Townshend, J.R. Empirical comparison of Landsat 7 and IKONOS multispectral measurements for selected Earth Observation System (EOS) validation sites. *Remote Sens. Environ.* **2003**, *88*, 80–99.
65. Ehlers, M.; Gaehler, M.; Janowsky, R. Automated techniques for environmental monitoring and change analyses for ultra high-resolution remote sensing data. *Photogramm. Eng. Remote Sens.* **2006**, *7*, 835–844.
66. Lu, D.; Hetrick, S.; Moran, E.; Li, G. Detection of urban expansion in an urban-rural landscape with multitemporal QuickBird images. *J. Appl. Remote Sens.* **2010**, *4*, 1–22.
67. Dare, P. Shadow analysis in high-resolution satellite imagery of urban areas. *Photogramm. Eng. Remote Sens.* **2005**, *71*, 169–177.
68. Cleve, C.; Kelly, M.; Kearns, F.R.; Moritz, M. Classification of the wildland–urban interface: A comparison of pixel- and object-based classifications using high-resolution aerial photography. *Comput. Environ. Urban Syst.* **2008**, *32*, 317–326.
69. Zhou, W.; Troy, A.; Grove, M. Object-based land cover classification and change analysis in the Baltimore metropolitan area using multitemporal high resolution remote sensing data. *Sensors* **2008**, *8*, 1613–1636.
70. Cadenasso, M.L.; Pickett, S.T. a.; Schwarz, K. Spatial heterogeneity in urban ecosystems: Reconceptualizing land cover and a framework for classification. *Front. Ecol. Environ.* **2007**, *5*, 80–88.
71. Trimble eCognition Developer 8.7.2; 2012; 262.
72. Linke, J.; McDermid, G.J. A conceptual model for multi-temporal landscape monitoring in an object-based environment. *IEEE J. Sel. Top. Appl. Earth Obs. Remote Sens.* **2011**, *4*, 265–271.
73. Haralick, R.; Shanmugan, K.; Dinstein, I. Textural features for image classification. *IEEE Trans. Syst. Man Cybern.* **1973**, *3*, 610–621.
74. Huth, J.; Kuenzer, C.; Wehrmann, T.; Gebhardt, S.; Tuan, V.Q.; Dech, S. Land cover and land use classification with TWOPAC: Towards automated processing for pixel- and object-based image classification. *Remote Sens.* **2012**, *4*, 2530–2553.
75. ESRI (Environmental Systems Resource Institute) ArcMap 10.1; 2011.
76. Breiman, L. Random Forests. *Mach. Learn.* **2001**, *45*, 5–32.

77. Cutler, D.R.; Edwards, T.C.; Beard, K.H.; Cutler, A.; Hess, K.T.; Gibson, J.; Lawler, J.J. Random forests for classification in ecology. *Ecology* **2007**, *88*, 2783–2792.
78. Timm, B.; McGarigal, K. Fine-scale remotely-sensed cover mapping of coastal dune and salt marsh ecosystems at Cape Cod National Seashore using Random Forests. *Remote Sens. Environ.* **2012**, *127*, 106–117.
79. R Core Team. *R: A Language and Environment for Statistical Computing*; R Foundation for Statistical Computing, Vienna, Austria, 2013.
80. Liaw, A.; Wiener, M. Classification and regression by randomForest. *R News* **2002**, *2*, 18–22.
81. Guisan, A.; Zimmermann, N.E. Predictive habitat distribution models in ecology. *Ecol. Modell.* **2000**, *135*, 147–186.
82. Moisen, G.G.; Frescino, T.S. Comparing five modelling techniques for predicting forest characteristics. *Ecol. Modell.* **2002**, *157*, 209–225.
83. Zimmerman, P.L.; Housman, I.W.; Perry, C.H.; Chastain, R.A.; Webb, J.B.; Finco, M.V. An accuracy assessment of forest disturbance mapping in the western Great Lakes. *Remote Sens. Environ.* **2013**, *128*, 176–185.
84. Gregory, R.; Failing, L.; Harstone, M.; Long, G.; McDaniels, T.; Ohlson, D. *Structured Decision Making: A Practical Guide to Environmental Management Choices*; Wiley-Blackwell: West Sussex, UK, 2012.
85. Antrop, M. Landscape change and the urbanization process in Europe. *Landsc. Urban Plan.* **2004**, *67*, 9–26.
86. Jensen, K.C. An Evaluation of Land Cover Change from 2006 to 2009 and the Effectiveness of Certain Conservation Land Use Tools Within Lake Washington/Cedar/Sammamish Watershed (WRIA 8) Riparian Buffers. Master's Thesis, University of Washington, Washington, DC, USA, 2012.
87. *ERDAS Imagine 2010 Field Guide* TM; 2010, 842p.

© 2015 by the author; licensee MDPI, Basel, Switzerland. This article is an open access article distributed under the terms and conditions of the Creative Commons Attribution license (<http://creativecommons.org/licenses/by/4.0/>).